

# **Mechanistic insights into the conversion of dimethyl ether over ZSM-5 catalysts: a combined temperature programmed surface reaction and microkinetic modelling study**

Toyin Omojola<sup>a,b,&\*</sup> and Andre C. van Veen<sup>b</sup>

<sup>a</sup> Department of Chemical Engineering, University of Bath, Claverton Down, Bath, BA2 7AY, UK

<sup>b</sup> School of Engineering, Library Road, University of Warwick, Coventry, CV4 7AL, UK

<sup>&</sup> Current address: Department of Inorganic Chemistry, Fritz-Haber-Institut der Max-Planck-Gesellschaft, D-14195 Berlin, Germany

\* Corresponding author: toyin.omojola@bath.edu

**Keywords:** transient kinetics, microkinetic modelling, TPSR, scaling relations, methanol, ZSM-5, dimethyl ether, propylene, active site engineering, periodic operation

## Abstract

Rates of adsorption, desorption, and surface reaction of dimethyl ether (DME) to olefins over fresh and working ZSM-5 catalysts of different Si/Al ratios (36 and 135) have been decoupled using a combination of temperature programmed surface reaction experiments and microkinetic modelling. Transient reactor performance was simulated by solving coupled 1D non-linear partial differential equations accounting for elementary steps occurring during the induction period based on the methoxymethyl mechanism on the zeolite catalyst, and axial dispersion and convection in the reactor. Propylene is the major olefin formed and scaling relations between activation energies of DME desorption and barriers of formation of methoxymethyl and methyl propenyl ether are observed. Six ensembles of sites are observed with a maximum of three adsorption/desorption sites and three adsorption/desorption/reaction sites. Barriers are generally higher over working catalysts than fresh catalysts. Activation energies of propylene formation of ca. 200 kJ mol<sup>-1</sup> are obtained corroborating direct mechanistic proposals.

## 1. Introduction

The growing propylene demand has prompted increasing investigations into its clean, secure and cost-effective production.<sup>1</sup> Methanol, obtained *via* biomass or organic process waste gasification and subsequent syngas liquefaction, can be used to meet these challenges. Subsequently, methanol can be converted to hydrocarbons, which can be tuned, depending on economic needs towards olefin<sup>2-4</sup>, aromatic<sup>5</sup> or gasoline<sup>6</sup> formation over zeolite and zeotype catalysts.

During the early stages of methanol-to-olefin (MTO) conversion over fresh catalysts, methanol adsorbs molecularly or dissociates upon adsorption on ZSM-5 catalysts giving surface methoxy species and water. Room temperature methoxylation has been observed over ZSM-5 catalysts.<sup>7,8</sup> Methanol could further react with these surface methoxy groups to give dimethyl ether (DME) with replenishment of the initial active site. DME adsorbs molecularly and/or dissociatively on the ZSM-5 catalyst leading to surface methoxy species and adsorbed methanol. The initial steps of methanol-to-olefin conversion involves an equilibration process of methanol, DME and water with surface methoxy species and molecularly adsorbed species acting as intermediates.<sup>9,10</sup>

Although dimethyl ether can be produced from methanol,<sup>11</sup> at high scale it can also be obtained from different fossil fuels, biomass and carbon dioxide and can be considered independently as an alternative process to the formation of olefins.<sup>12,13</sup> However, higher water content is obtained during MTO conversion in comparison to dimethyl ether to olefins (DTO) conversion leading to faster deactivation by coke in the latter (DTO) under atmospheric conditions.<sup>14,15</sup>

At steady-state under atmospheric conditions, it is well established that a “hydrocarbon pool” forms and operates through a dual-cycle mechanism over the working catalyst.<sup>16-20</sup> This dual-cycle consists of an alkene and an aromatic cycle. Primary olefins, that is ethylene and/or propylene, are surface methylated by methanol and/or DME to give higher homologues which crack to establish the olefin cycle.<sup>10,21</sup> The higher olefin homologues ( $C_{6+}$ ) undergo hydrogen transfer and cyclisation to form aromatics.<sup>22</sup> The initial aromatics are surface methylated by

methanol and/or DME giving higher aromatics and dealkylate to produce olefins (ethylene and/or propylene) and lower aromatics.<sup>10</sup> Differences in the mechanism have been observed with Si/Al ratio.<sup>23</sup> The product distribution over ZSM-5 catalysts can be tuned towards olefin formation at relatively low pressures and high temperatures.<sup>2,24,25</sup>

Although the initial steps and the steady-state processes are increasingly well defined under atmospheric conditions, the conversion of these initial species (methanol, DME and water) to the first hydrocarbon pool species is not well established. The formation of the first C-C bond during the induction period of methanol-to-olefin formation is highly debated. Numerous direct mechanisms have been proposed for the formation of the first C-C bond, namely the carbene mechanism<sup>26-30</sup>, multiple analogues of the oxonium<sup>31</sup> and methane-formaldehyde mechanism<sup>32</sup>, the methyleneoxy mechanism<sup>33</sup>, surface methoxy groups<sup>29,34-36</sup> and the methoxymethyl cation mechanism.<sup>37</sup> The experimentally and theoretically verified methoxymethyl mechanism allows for the formation of methoxymethyl cation, methyl propenyl ether, and dimethoxyethane as the first C-C bond in the formation of propylene.<sup>37,38</sup> Furthermore, the transformation of active sites during the induction period and transition regime is also not completely understood.<sup>39</sup> This dual problem, namely that of the evolution of the reaction network (mechanism responsible for the first C-C bond) and that of the transformation of active sites can be solved simultaneously by observing the thermal evolution of the fresh catalyst during reaction. This is investigated here by conducting temperature programmed surface reaction (TPSR) experiments with DME over ZSM-5 catalysts. TPSR was first introduced by McCarty and Wise<sup>40</sup> to decouple the carbon species formed on an alumina-supported nickel methanation catalyst. Mechanistic insights can be gleaned through multiscale microkinetic modelling by fitting a mechanism that allows for decoupling of elementary steps of adsorption, desorption, and surface reaction and their relationship to the dispersion and convection through the reactor. Parameters obtained in this study by fitting a reaction mechanism complement other first principle methods applied to transient kinetics.<sup>41</sup>

Temperature programmed surface reaction is a type of transient operation. The concept of using unsteady-state operation to enhance performance is not new in chemical

engineering. There has been an increasing interest in designing catalytic reactors operating under transient conditions since the concept of periodic operation was first formally introduced in the late 1980s by Haure et al.<sup>42</sup> Modulation of activity has been previously accomplished by introducing an extra component, which can help catalyst regeneration and prevent build-up of inhibitors in the catalyst. By applying periodic forcing, one can potentially increase the yield and selectivity of catalytic reactions.<sup>43-45</sup> Despite this knowledge, our understanding of the complex underlying process that occurs at different time and length scales and governs catalytic processes during unsteady-state conditions is still relatively poor.<sup>46</sup>

In this work, we conducted temperature programmed surface reaction experiments in a temporal analysis of products reactor and multi-scale microkinetic modelling studies of DME over fresh and working ZSM-5 catalysts of different Si/Al ratios to gain further understanding of: (1) barriers associated with the methoxymethyl mechanism occurring during the induction period over ZSM-5 catalysts at meso-scale level and (2) the barriers associated with changing the nature of the catalyst from its fresh state to working state. Previous work by Li et al.<sup>37</sup> unveiled the barriers over SAPO-34 catalysts using density functional theory calculations. However, our work obtains the barriers over ZSM-5 catalysts using meso-scale microkinetic models (allowing for comparisons) and is amenable to MTO process design calculations. Li et al.<sup>37</sup> did not investigate the effects of the nature of the catalyst (i.e. fresh or working) which is of utmost importance given that ZSM-5 catalysts are well established to have high stability due to their 3D pore architecture<sup>47</sup>. The fresh catalysts were investigated as it evolves from its initial state to a working state under transient TPSR conditions. Working catalysts, used for methanol to olefin conversion *a priori*, were also investigated as it evolves from one working state to another working state. We observed an induction period and a transition regime during the transformation of the fresh catalysts to the working catalyst and the addition of precursors leads to the reduction of this induction period and alters the transition regime during transient kinetic studies.<sup>48,49</sup>

Dimethyl ether was chosen as it is advantageous towards higher propylene selectivity.<sup>50</sup> ZSM-5 catalysts are used due to their high stability.<sup>47</sup> Thus, having fixed stability

and product selectivity descriptors, activity descriptors can be investigated. Step response experiments were also conducted under flow conditions in a temporal analysis of products reactor that operates under low pressure conditions. This also allows for the tuning of the product distribution towards olefin formation.<sup>48</sup> In addition to our previous work,<sup>48</sup> microkinetic simulations on the first cycle of the step response experiments allowed us to understand if there is agreement between the carbene mechanism and experimental data. Furthermore, the microkinetic modelling studies allow for a hierarchical bridge between the reaction kinetics of elementary steps on the particle scale, and dispersion and convection on the reactor scale. We note that this temperature programmed surface reaction approach complement our previous studies through a reductionist approach that aimed to decouple adsorption, desorption, activity and diffusion through an individual combination of temperature programmed desorption<sup>51</sup>, step response<sup>48,49</sup> and quasi-elastic neutron scattering<sup>52</sup> studies to probe the formation of primary olefins from oxygenates over fresh and working ZSM-5 catalysts. In this TPSR work, we reveal scaling factors between desorption energies of DME and the barriers of formation of key intermediates (methoxy methyl species and methyl propenyl ether) involved in propylene formation over ZSM-5 catalysts and mechanistic insights into how activity can be improved by process modulation and active site engineering.

## 2. Experimental

### 2.1. Materials

All experiments were carried out with 10 mg of ZSM-5 catalysts of different Si/Al ratios (36 and 135), here referred to as ZSM-5 (36) and ZSM5 (135) respectively. ZSM-5 (36) and ZSM-5 (135) catalysts were obtained from BP chemicals. The ammonium form of the zeolites was pressed, crushed, and sieved to obtain particles sizes in the range of 250 – 500  $\mu\text{m}$ . Anhydrous DME (99.999%) and argon (99.999%) were obtained from CK special gases Ltd.

### 2.2. Temporal Analysis of Products (TAP) reactor

Temperature programmed surface reaction experiments were conducted in a temporal analysis of products reactor. The set-up allowed for zeolite decomposition under vacuum conditions. 5 vol% DME (balance argon) was fed into the TAP system using the continuous feeding valves. The TAP reactor will be introduced here briefly although there are excellent reviews on the TAP reactor.<sup>53-56</sup> The TAP reactor<sup>53</sup> consists of three chambers in series: (a) the reactor chamber, (b) the differential chamber and (c) the detector chamber. The pressure at the inlet to the reactor chamber is *ca.* 1000 Pa under continuous flow. The pressure at the exit of the reactor chamber is maintained at  $10^{-5}$  Pa and at the end of the differential chamber is  $10^{-6}$  Pa and in the detector chamber, where the quadrupole mass spectrometer (QMS) is housed, is  $10^{-7}$  Pa. The active catalyst bed length is short (2 mm) compared to the overall bed length of 25 mm (consisting of a configuration of quartz wool/quartz beads/active catalyst bed/quartz beads/quartz wool) to minimize any pressure differences. The packed bed housed in an inert quartz tube was placed in a metallic body to provide further mechanical stability.<sup>57</sup>

### 2.3. Characterisation

The characterisation of the catalyst samples has been reported before.<sup>49,51</sup> The samples were studied by X-ray diffraction (XRD) with a Bruker D5005 diffractometer using Cu  $K_{\alpha}$  radiation equipped with standard Bragg-Brentano geometry and a diffracted beam graphite monochromator. The samples obtained were compared with reference XRD data for

crystallinity and further characterization. The morphological features of the zeolites were characterized using a Carl Zeiss sigma series Field Emission Scanning Electron Microscope. Nitrogen physisorption studies were carried out on a Micromeritics 2020 unit. The samples were degassed by heating to 673 K under vacuum ( $10^{-6}$  mbar) for 12 h. After degassing, the weight of the dried sample was determined. Subsequently, the sample was cooled to 77 K and liquid nitrogen was adsorbed at increasing partial pressures.

The ZSM-5 (36) catalyst has a crystallite size of  $0.33 \pm 0.05$   $\mu\text{m}$ , an apparent BET surface area of  $410 \text{ m}^2 \text{ g}^{-1}$ ,  $117 \mu\text{mol g}^{-1}$  of Brønsted acid sites (BAS),  $80 \mu\text{mol g}^{-1}$  of Lewis acid sites (LAS), and a BAS/LAS ratio of 1.5. The ZSM-5 (135) catalyst has a crystallite size of  $0.78 \pm 0.07$   $\mu\text{m}$ , an apparent BET surface area of  $358 \text{ m}^2 \text{ g}^{-1}$ ,  $78 \mu\text{mol g}^{-1}$  of BAS,  $30 \mu\text{mol g}^{-1}$  of LAS, and a BAS/LAS ratio of 2.6.<sup>51</sup>

#### 2.4. Temperature Programmed Surface Reaction (TPSR)

Before the start of each experimental series, the ammonium form of the catalysts was decomposed at  $15 \text{ K min}^{-1}$  under vacuum conditions up until 723 K and held for 30 min before subsequently cooled down at  $25 \text{ K min}^{-1}$  to room temperature. The vacuum reactor was baked before the experimental series for more than 48 h to evacuate hydrocarbon residues.

Over ZSM-5 (36) and (135), a baseline of argon flow over the fresh and working ZSM-5 catalysts was established, then TPSR was carried out by saturating the catalyst with 5 vol% DME (balance argon) at  $10^{-8} \text{ mol s}^{-1}$  and thereafter subjecting the catalyst immediately to a linear temperature ramp of  $15 \text{ K min}^{-1}$  up until 723 K. A sample TPSR profile of DME is given in section S1 of the supplementary information.

The methodology used to obtain the working zeolites has been given before.<sup>51</sup> For brevity here, the ammonium form of the ZSM-5 catalysts of Si/Al ratios of 36 and 135 were calcined with 30%  $\text{O}_2/\text{N}_2$  in a fixed bed reactor (4 mm I.D, 6 mm O.D) at  $10 \text{ K min}^{-1}$  until 723 K and held there for 30 min before subsequently cooled at  $25 \text{ K min}^{-1}$  under nitrogen gas to 673 K, where they were subjected to 1.3 vol% of methanol at a flowrate of  $10 \text{ mL min}^{-1}$ .

Gaseous products were monitored using an online GC-FID equipped with an Equity-1 capillary column. Samples were withdrawn after 2 h time on stream from the fixed bed reactor.

The effluent was monitored using the QMS housed in the detector chamber. The response of the QMS, placed in the detector chamber, was calibrated by passing continuous streams of various gases (methanol, DME, water, ethylene, propylene) in argon over an inert quartz bed with particle diameter between 355 – 500  $\mu\text{m}$ . The inert quartz bed was of similar bed length to the bed of catalyst and quartz used in the standard TPSR experiments. From the calibration data, sensitivity coefficients were obtained and used to obtain mole fractions of the respective constituents. Argon was monitored at  $m/e = 40$ ,  $\text{CH}_3\text{OH}$  at  $m/e = 31$ , DME at  $m/e = 45$ ,  $\text{H}_2\text{O}$  at  $m/e = 18$ ,  $\text{C}_2\text{H}_4$  at  $m/e = 27$ ,  $\text{C}_3\text{H}_6$  at  $m/e = 41$ . Previous DME step response work over ZSM-5 catalysts in our laboratory showed that ethylene and butene selectivities were negligible at 573 K under vacuum conditions. Subsequent deconvolution allowed for the subtraction of minor fragment of other species from main species. The quantification procedure is detailed in section S2 of the supplementary information. The low base pressure, that is  $10^{-7}$  Pa in the detector chamber, allows for high detection sensitivity necessary for quantitative analysis.

The temperature programmed surface reaction studies of DME over fresh and working ZSM-5 catalysts were compared to temperature programmed desorption (TPD) studies of DME over the same catalysts. TPD studies of DME over fresh and working ZSM-5 (36) and (135) catalysts were performed and analysed using a microkinetic model given in a previous publication.<sup>51</sup> During the TPD studies, 10 mg of the ammonium form of the ZSM-5 (36) and ZSM-5 (135) catalysts were pressed, crushed and sieved to obtain particle sizes in the range of 250 – 500  $\mu\text{m}$ . The active catalyst was packed between two quartz wool plugs with the active catalyst zone of 2 mm, in a bed length of 25 mm. The experimental set up allowed for the formation of active H-form of the zeolite catalyst by decomposition of the ammonium form under vacuum conditions. Probe molecules (5 vol% DME, balance argon) were fed using continuous feeding valves. Over ZSM-5 (36) and ZSM-5 (135) only DME was observed in the desorption profile.

We note here that over the same catalysts and using similar molar flow rates and temperatures, we observe no deactivation with time on stream over our experimental timescale.<sup>49</sup>

## 2.5. Microkinetic simulations

A non-ideal plug flow reactor model was used to simulate the TPSR experiments. This model accounting for adsorption, desorption, and surface reactions as well as dispersion and convection was constructed using an in-house MATLAB code (MTOTAPCAT).

Although TPSR experiments at low partial pressures and high linear velocity are unlikely to be affected by dispersion, penetration of the zeolite pore system in the radial dimension would effectively lead to the need of accounting for a second reactor dimension. In an initial stage of code development, explicitly accounting for a 2D geometry problem in a transient kinetic problem involving many gaseous and surface species proved to be computationally expensive and issues with mismatching length scales could contribute to numerical instability. Therefore, we opted for a workaround strategy using an axial dispersion term only. Furthermore, preliminary calculations show that the crystallite sizes are small enough to ensure optimum effectiveness factors. Coppens et al.<sup>58</sup> showed that the ethylation of benzene over ZSM-5 particles requires a zeolite crystallite size of 240 nm for an effectiveness factor of >95%. We obtain hardly any formed olefins with the larger crystallites of ZSM-5 (135) between 300 and 723 K at a heating rate of 15 K min<sup>-1</sup> so we can't consider its influence on propylene formation, and the ZSM-5 (36) crystallite size is small enough (330 nm) to guarantee an effectiveness factor of >90% according to Figure 2 in ref.<sup>58</sup> However, we do note that methanol-to-olefin reaction chemistry differs from the ethylation of benzene over ZSM-5 catalysts and further preliminary reaction-diffusion simulations are required to ascertain the influence of the pore penetration depth across the zeolite crystal. Nonetheless, an effectiveness factor greater than 90% suffices to ensure the rigour in our lumped axial dispersion surrogate model (without the radial dimension). Addition of anomalous diffusion may help in better correspondence between experiment and model. The inclusion of surface mobility of adsorbed species may further help improve our correspondence between experiment and model. However, these improvements would likely lead to an increased number of parameters which would affect the confidence interval but also increased

computational time. Modelling was conducted with as few parameters as possible while still maintaining some physicochemical meaning of the description of the DME TPSR profiles.

The MTOTAPCAT code allowed for the estimation of pre-exponential factors and activation energies of desorption, reaction, and formation of primary olefins from DME over fresh and working ZSM-5 catalysts. In the MTOTAPCAT code, desorption rate parameters are fitted, and adsorption rates are calculated. Here, adsorption, desorption and surface reaction rates can be extracted directly from the parameters.

A kinetic scheme based on a methoxymethyl pathway<sup>37,38</sup> involving the methoxymethyl cation, dimethoxyethane and methyl propenyl ether was used to describe the formation of primary olefins. Previously, we showed that this pathway gives the closest agreement (in comparison to methane-formaldehyde, carbon monoxide routes) with transient kinetic data during the induction period.<sup>48</sup> We note here that this pathway allows for the formation of the first C-C bond in the induction period and does not account for either a transition regime to steady-state (where the hydrocarbon pool dominates) or the formation of the hydrocarbon pool during steady-state. Moreover, there exists no proof in the archived literature of a “hydrocarbon pool” existing under sub-vacuum or vacuum conditions. Although, the methoxymethyl pathway was observed over SAPO-34 catalysts<sup>37</sup> and catalyst structure plays a major role in the product obtained<sup>59</sup>, we envisage that the use of this pathway over ZSM-5 catalysts would allow for mechanistic comparisons with archived literature. Further comparison to the carbene mechanism is described below (see section S8 in the supplementary information). The kinetic model was solved according to equations 2.1 and 2.2 (assuming a first order reversible process):<sup>60</sup>

**Gas**

$$\varepsilon_b \frac{\partial C_{i,g}}{\partial t} = D_{i,e} \frac{\partial^2 C_{i,g}}{\partial z^2} - u \frac{\partial C_{i,g}}{\partial z} - \Gamma_t S_v (1 - \varepsilon_b) (k_a c_i - k_d \theta_{iz}) \quad (2.1)$$

**Surface**

$$\frac{\partial \theta_i}{\partial t} = k_a c_i - k_d \theta_{iz} \quad (2.2)$$

where  $k_a$  is the adsorption coefficient ( $\text{m}^3 \text{mol}^{-1} \text{s}^{-1}$ ),  $c_i$  is the concentration of gas phase component,  $i$  ( $\text{mol m}^{-3}$ ),  $\varepsilon_b$  is bed porosity;  $u$  is the superficial velocity,  $\text{m s}^{-1}$ ;  $z$  is the bed length,  $\text{m}$ ;  $t$  is time,  $\text{s}$ ;  $\Gamma_t$  is the concentration of active sites per unit surface area of catalyst ( $\text{mol m}_{\text{cat}}^{-2}$ ) and  $S_v$  is the catalyst surface area per unit volume ( $\text{m}_{\text{cat}}^{-1}$ ),  $k_d$  is the desorption rate coefficient ( $\text{s}^{-1}$ ) and  $\theta_i$  is the fractional surface coverage of the adsorbed specie.

We note here that the methodology presented here is different from our previous work<sup>48</sup>. In our previous step response study, the first cycle is investigated through a one-site model with respect to time at a constant temperature. In our current TPSR study, to obtain activation energies, a temperature ramp is applied. This allows for acquisition of activation energies as the gas and surface equations (equations 2.1 and 2.2 respectively) are solved with respect to temperature (using the fixed heating rate) and with several sites participating. In this TPSR study, we obtain novel results on which sites are activity promoting within a given range of temperatures. The results are applicable to catalyst design specialists who could isolate the activity promoting site (as discussed below) and improve on the MTO process. This particular information is not obtainable from our previous step response studies. Thus, the TPSR/microkinetic modelling methodology applied provide, hitherto not attained, improved understanding of the MTO process.

This study is one among a series of studies<sup>48,49,51,61</sup> conducted in our laboratory to get mechanistic information into the formation of the primary C-C bond during MTO conversion using the temporal analysis of products reactor. The dispersion coefficient,  $D_{i,e}$  ( $\text{m}^2 \text{s}^{-1}$ ), bed

porosity (-) and superficial velocity ( $\text{m s}^{-1}$ ) were fixed according to our previous step response experiments<sup>48</sup> conducted under similar conditions.

**Initial condition:**  $t = 0$ ,  $C_{i,g} = 0$ ,  $\theta_i = 0$  (except  $\theta_{\text{DME}} = 1$ ).

**Boundary conditions:**  $C_i(t, 0) = C_{i,j} = C_{\text{DME},j}$  ( $C_{\text{others},j} = 0$ ),  $\theta_{\text{DME},j} = 1$ ,  $\theta_{\text{others},j} = 0$ .

$$C_i(t, J); C_{i,j} = C_{i,j-1}; \theta_{i,j} = \theta_{i,j-1}$$

Backward differencing was applied to the convection term in the partial differential equation above. To ensure numerical stability, the Courant-Friedrichs-Lewy (CFL) condition<sup>62</sup> was satisfied:

$$CFL = \left| a \frac{\Delta t}{\Delta z} \right| \leq 1 \quad (2.3)$$

where  $a = u/\varepsilon_b$ . The time domain was divided into 400,000 strips and the space domain into 5 strips. This led to a reduction in computational time while still maintaining the CFL criterion. We do note here that there are other methods using a distributed function of the activation energy in archived literature.<sup>63-65</sup> However, such regularization methods have been shown to lead to negative parts of the distributed function which lack physical meaning. Thus, the model above was used with good confidence in the physical meaning of the estimated parameters.

The sum of square error (SSE) between experiment and model was obtained according to<sup>66,67</sup>:

$$SSE = \sum_{n=1}^{N_c} \sum_{m=1}^{N_d} w_{n,m} (Y_{n,m}^{obs} - Y_{n,m}^{cal})^2 \rightarrow \min \quad (2.4)$$

where:

n component number

m observation number

$N_c$  total number of components

$N_d$  total number of observations

$w_{n,m}$  weighting factor of the m-th observation of component n

$Y^{obs}$  experimental data

$Y^{cal}$  model data

The initial parameter estimates were improved greatly by reducing the sum of squares error between model and experiment (equation 2.4). Parameter optimisation through the minimisation of the sum of square error using an “fminsearch” function was carried out in the MTOTAPCAT code for over 150 h in each case. The “fminsearch” function uses a Nelder-Mead simplex algorithm as described by Lagarias et al.<sup>68</sup> In equation 2.4, the weighing factors were calculated as:<sup>69</sup>

$$w_{n,m} = \frac{1}{\sum_{m=1}^{x_{exp}} Y_{n,m}} \quad (2.5)$$

where  $x_{exp}$  is the total number of experimental points. The expression allows that the minority species in the reaction medium have a higher weighing factor. After parameter optimisation, each parameter was checked and validated (along with the sensitivity analysis) for physical significance.

In an effort to obtain confidence intervals for the estimated parameters, a nearly singular matrix was obtained as the determinant of the  $(J^T \cdot J)$  is close to zero (where J is the Jacobian matrix). This was due to the exceptionally low differences in the outlet molar flowrates when a 1% change is applied to the estimated parameters. Molar flow rates are of the order of  $10^{-8}$  mol  $s^{-1}$ . Differences in a 1% change resulted in changes of  $10^{-12} - 10^{-14}$  mol  $s^{-1}$  leading to badly conditioned matrixes in the estimation of the confidence intervals according to ref.<sup>67</sup>

We considered five gaseous species (methanol, DME, water, ethylene, and propylene) and eight surface species (adsorbed methanol, adsorbed DME, adsorbed water, surface methoxy specie, methoxy methyl specie, methyl propenyl ether, adsorbed dimethoxyethane adsorbed propylene) in this reduced model. However, there are greater than 90 species and 200 products including isomers formed in the hydrocarbon pool. Previous contributions on steady-state kinetics considered elementary steps of the same family group.<sup>70,71</sup> The TAP reactor allows the decoupling of elementary steps of adsorption, desorption, and reaction during hydrocarbon conversions and grouping reaction steps does not allow for its full functionality.<sup>56</sup> Also, consideration of all elementary reactants and products during transient

conditions is a formidable task even on modern workstations. Limitations due to computational costs and time required for the solution of coupled partial differential equations allowed for the focus on the transformation of major reactants and products.

### 3. Results

#### 3.1. Comparison between TPD and TPSR profiles

A comparison of TPD and TPSR profiles shows that the temperature of the highest intensity for adsorption/desorption/reaction for the DME TPSR profiles are slightly higher than the temperature of maximum intensity for DME adsorption/desorption on fresh and working ZSM-5 (36) catalysts. However, over ZSM-5 (135) catalysts, the temperature of maximum intensity stays relatively constant for fresh and working catalysts across TPD and TPSR experiments. We observe that during the TPSR of DME over ZSM-5 (36) or (135) catalysts, some low temperature sites are more activated than in the TPD profiles over ZSM-5 (36) and (135) catalysts. We observe low temperature peaks and also observe high temperature shoulders for the TPSR plots, lower than the starting intensity of the DME profiles, possibly signifying some solid-gas reactions. In the TAP reactor, gas-solid reactions are prevalent at near vacuum conditions and in porous structures.<sup>56</sup> We observe that above 600 K, the removal of the species in the case of the TPSR profiles is slowed down by surface reactions in comparison to the TPD profiles. This is evidenced by the longer tails observed in the TPSR profiles. This is also more prevalent over ZSM-5 (36) catalysts. Mechanistic analysis of the TPD profiles using a microkinetic model has been given in ref.<sup>51</sup> We note here an important difference in the catalyst history during the TPD and TPSR studies. During the TPD studies, after establishing a baseline, the catalyst was saturated with 5 vol% DME (balance argon). 100 vol% argon was then passed through the bed to evacuate excess DME on the catalyst surface. Thereafter, a linear temperature ramp of 15 K min<sup>-1</sup> was applied to the catalyst to facilitate desorption of DME. In contrast, during the TPSR experiments, after establishing a baseline and saturating the catalyst with 5 vol% DME (balance argon), a linear temperature ramp of 15 K min<sup>-1</sup> was applied immediately. Figure 1 shows the TPD and TPSR profiles from the beginning of the application of that linear temperature ramp.

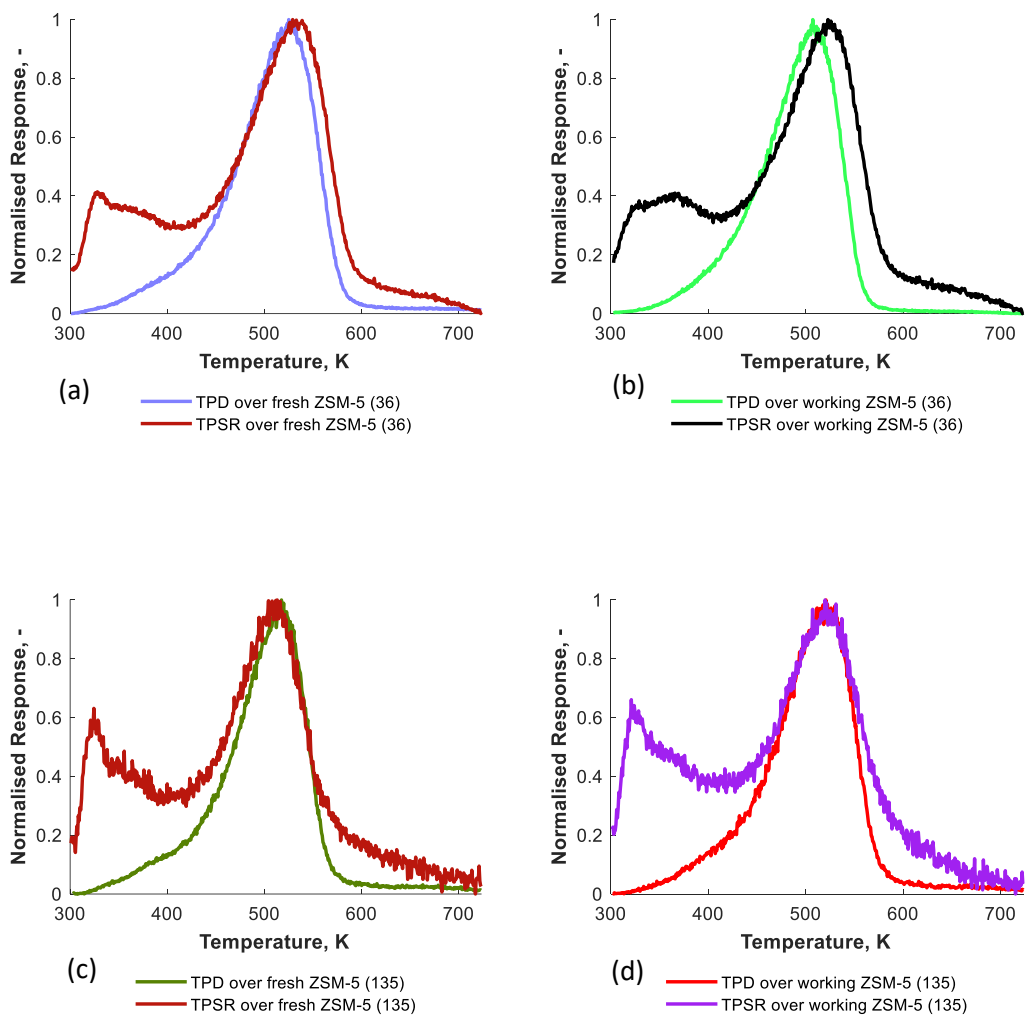


**Figure 1:** A comparison between DME TPD and DME TPSR profiles over fresh and working catalysts

### 3.2. Temperature programmed surface reaction profile analysis

Methanol forms at ca. 523 K, while propylene forms at ca. 673 K when TPSR of DME is carried out over fresh and working ZSM-5 (36) catalysts. Over ZSM-5 (135) catalysts, while methanol forms at 573 K, propylene formation is negligible in the temperature range between 300 – 723 K and at 15 K min<sup>-1</sup>. This is probably due to the lower strength of Brønsted acid sites on ZSM-5 (135) catalysts requiring higher temperatures for propylene formation. Moreover, the selectivity to ethylene during the TPSR of DME over ZSM-5 (36) and (135) catalysts is also negligible within the experimental temperature range. As a result, ethylene is not plotted in Figures 2-5, but shown in section S3 of the supplementary information.

We uncovered three adsorption sites (LT, MT, HT) during the temperature programmed desorption of DME over ZSM-5 (36) catalysts and two adsorption sites over ZSM-5 (135) catalysts.<sup>51</sup> In comparison, in tables S4 and S5 (sections S4 and S5 of the supplementary information), six ensembles of binding/active sites are required for adsorption, desorption and surface reaction during the temperature programmed surface reaction of DME over the ZSM-5 catalysts. These six ensemble sites relate to more low temperature TPSR activated sites and high temperature TPSR shoulders compared to the TPD profiles given over the same catalysts in our previous work. Of these six ensembles of binding sites, three were associated with adsorption and desorption and the remaining three sites had surface reaction or the generation of intermediates depicting the emergence of reaction associated with them (tables S4 and S5 of the supplementary information). These six ensembles of active sites were first determined through a combination of the species balance equations (equations 2.1 and 2.2 respectively) used to represent the TAP reactor and the methoxymethyl kinetic scheme (tables S4 and S5 of the supplementary information) used to determine the reaction pathways. Further analysis using the ORIGINPRO<sup>®</sup> software for fitting gaussian distribution curves to the TPSR profiles show confirmation of the six ensembles. Figure S7.1 in section S7 of the supplementary information shows the analysis obtained for the DME TPSR profile over working ZSM-5 (36) catalysts.

The rate parameters are dependent on the ZSM-5 zeolite. Substituting, for instance, the site densities of ZSM-5 (36) into ZSM-5 (135) and keeping the rate parameters the same as in ZSM-5 (135) does not reproduce the TPSR of DME profile over ZSM-5 (36) catalysts. Although each active/binding site can be tuned appropriately, each site must co-operate to reproduce the overall TPSR profile.<sup>72</sup> This concept of site cooperation has been previously identified before.<sup>73,74</sup> Consequently, the concept of a single site mechanism that spans the temperature range of 300 – 723 K is eliminated.

In our previous work<sup>48</sup>, we compared nine pathways for the initial C-C bond formation based on methane-formaldehyde, carbon monoxide and methoxymethyl pathway. Of these nine pathways, the pathway involving dimethoxyethane gives the best agreement between experiment and model over ZSM-5 catalysts. Over SAPO-34 catalysts, this pathway produced energetically feasible routes towards ethylene and propylene formation<sup>37</sup>. Thus, based on our studies and archived literature<sup>37,38</sup>, our kinetic model employing this specific kinetic scheme is justified. Furthermore, the method of Hunger and Hoffmann<sup>63,75,76</sup> which describes the heterogeneity of active sites by linear or logarithmic variation of activation energies of desorption of species with coverage while reaction barriers remained constant was tested and proved unreliable for our specific temperature programmed surface reaction analysis. Hunger and Hoffman<sup>63,75,76</sup> obtained simulation results for a relatively simple case - two gas phase and adsorbed species. This is vastly different from the complex mechanisms occurring during methanol to olefin conversion. Moreover, the method of Hunger and Hoffmann<sup>63,75,76</sup> introduces more parameters describing the linear or logarithmic variation of activation energies of desorption, which leads to the overall lack of confidence in the experimental description. Rather than one-site, we observed the site cooperation across temperatures to re-produce the TPSR profile.

The model agrees with experimental data over ZSM-5 (135) and ZSM-5 (36) catalysts. It is important to note that we have only represented the species with substantial concentrations in Figures 2-4. As a result, ethylene is not included in the main article but given in the supplementary information (see section S3). Four experimental data sets given by

Figures 2-5 have been used for estimation of four sets of parameters across six different sites. The DME TPSR profile over fresh and working ZSM-5 (135) catalysts were each represented by 60 parameters. The DME TPSR profile over fresh and working ZSM-5 (36) catalysts were each represented by 83 parameters. Each TPSR profile has a minimum of 500 transient data points per gas phase specie measured and ensures a high degree of confidence in the estimated parameters.<sup>67</sup> Dispersion coefficients of each of the five gas species and velocity through the reactor were estimated in agreement with our previous studies.<sup>48</sup> We expect that inclusion of anomalous diffusion (r-direction) may improve the model but this will increase the number of parameters to be estimated considering the number of sites and the number of gas species and may lead to a loss of physicochemical meaning of the estimated parameters.

The formation of propylene involves the transformation of the educt i.e. methanol or dimethyl ether first to an equilibrium mixture of methanol, DME and water and surface intermediates such as surface methoxy groups. These species are transformed first to primary olefins (ethylene, propylene) in an induction period. These primary olefins are then transformed *via* a transition regime to a *final regime* which dominates at steady state. Under atmospheric conditions, this *final regime* is controlled by the hydrocarbon pool mechanism. Under vacuum conditions, there exists no proof of the dominance of a hydrocarbon pool. Nonetheless, an S-shaped propylene profile that follows a crystal nucleation mechanism has been observed under close to vacuum conditions, highlighting the induction period, transition-regime and steady-state stated above.<sup>48,49</sup> We note here that the reaction mechanism employed in our microkinetic model i.e. the methoxymethyl mechanism explains accurately only the induction period as shown in Figures 2 and 3 for ZSM-5 (135). However, as shown in Figures 4 and 5 over ZSM-5 (36), methanol is produced steadily above 600 K suggesting that the inclusion of transition regime chemistry and steady-state chemistry is necessary to accurately describe the experimental profiles. However, until now there exists no proof of a dominating hydrocarbon pool mechanism under vacuum or close to vacuum conditions. We also anticipate that inclusion of more than 90 species and 200 species may increase the

computational costs. DME Parity plots given in Figures S6.1-S6.4 portray a high confidence in the model as shown in section S6 of the supplementary information.

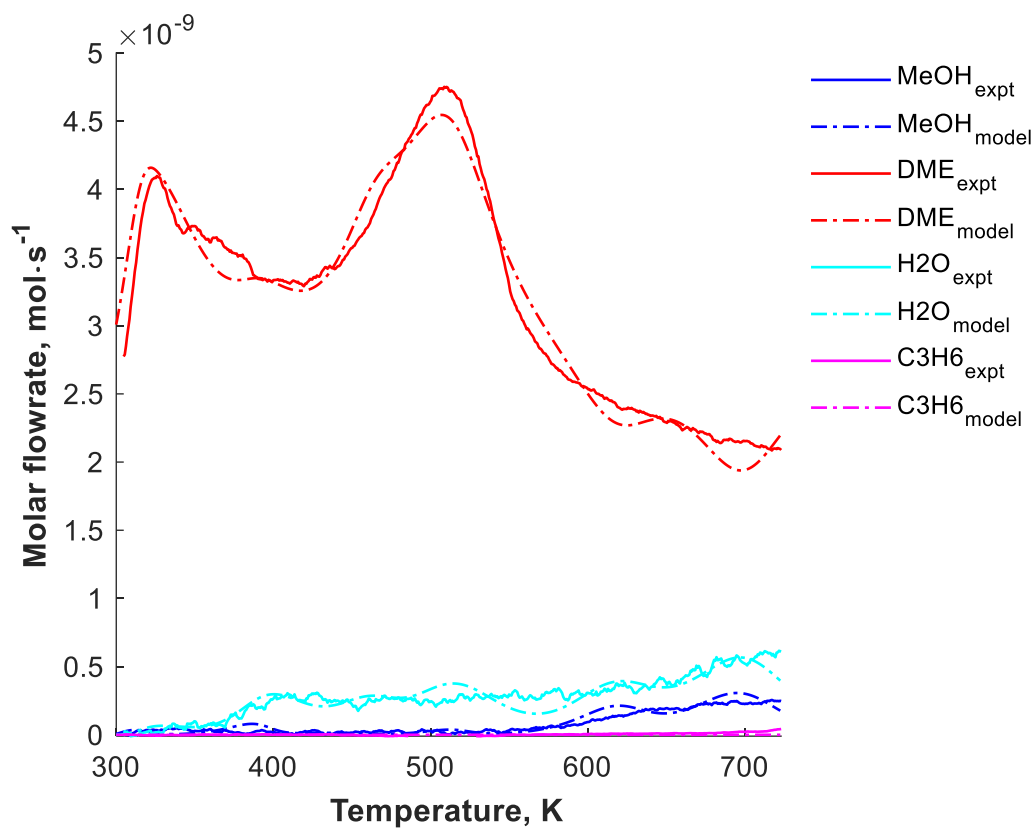


**Figure 2:** TPSR experiments with 5 vol% DME inlet feed over fresh ZSM-5 (135) catalysts

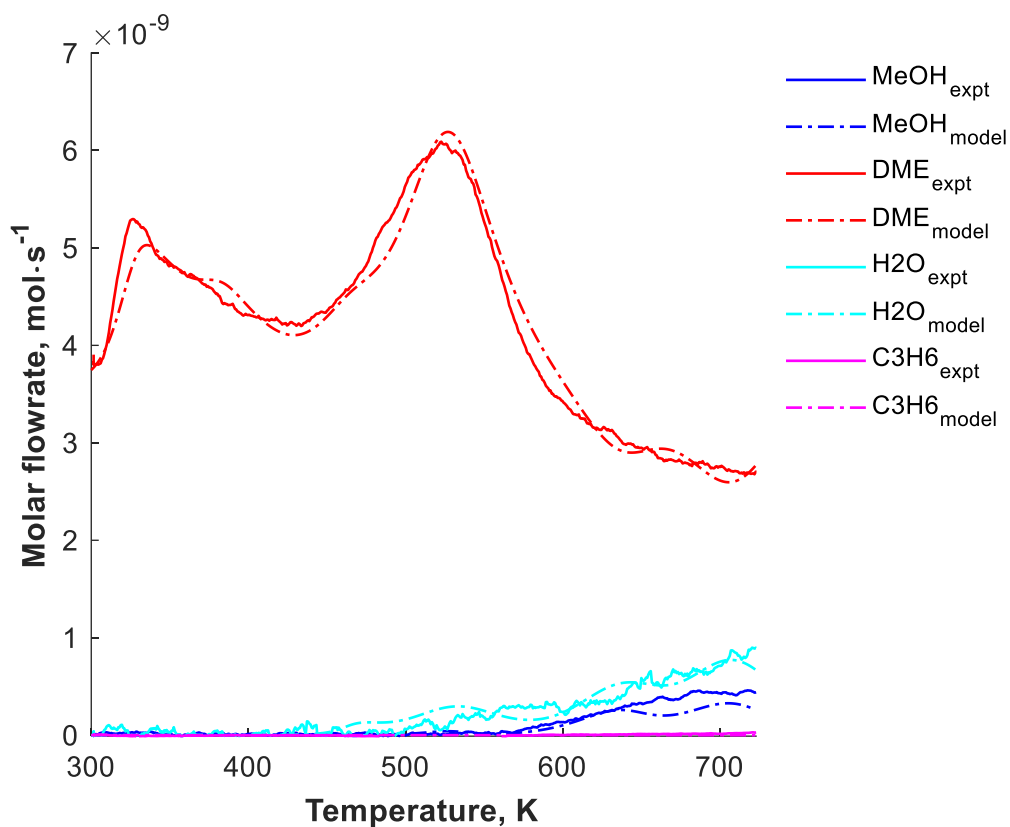
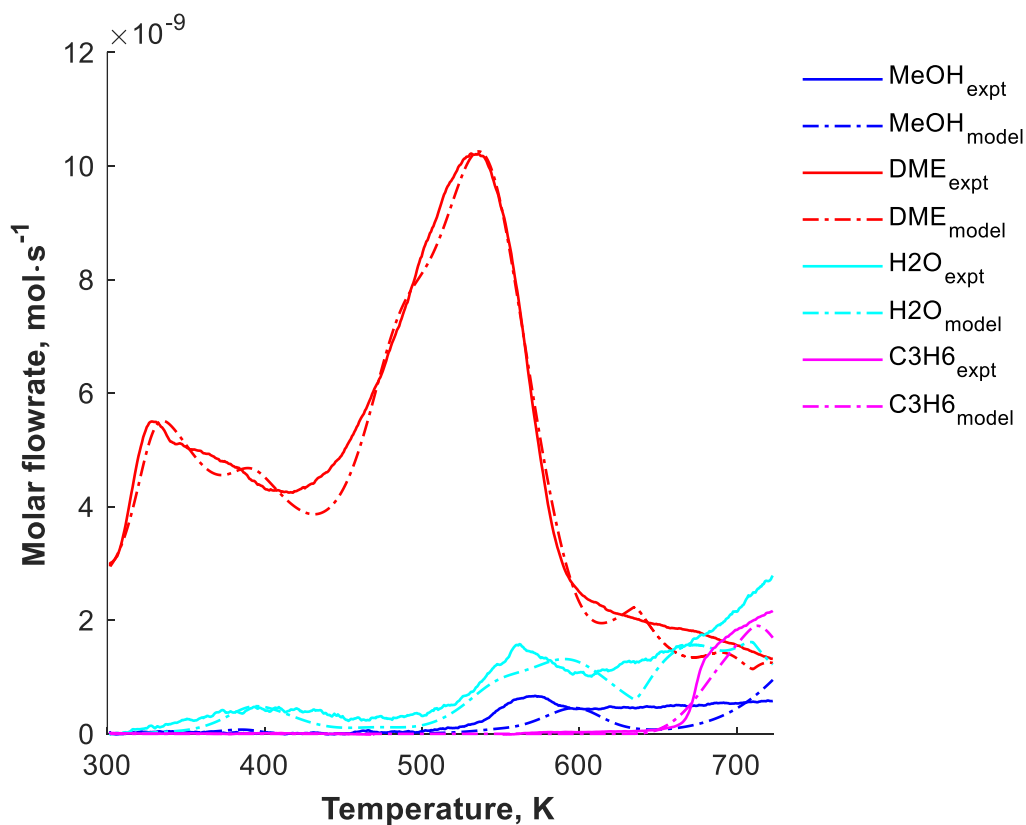
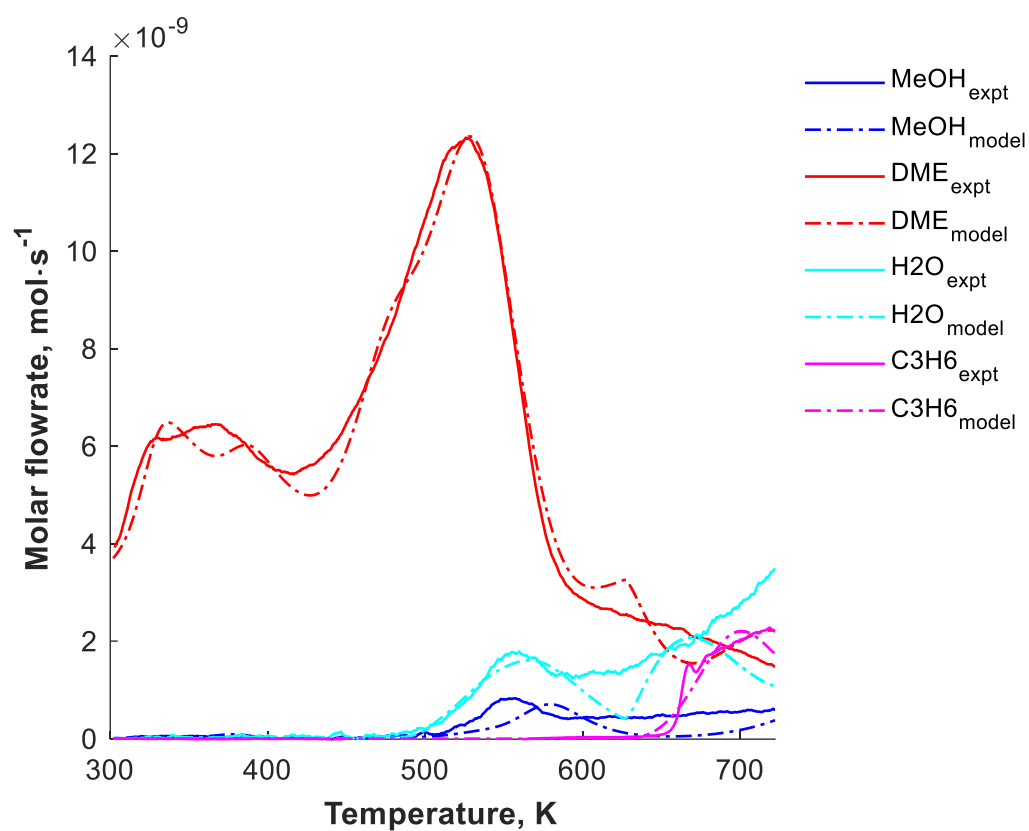


Figure 3: TPSR experiments with 5 vol% DME inlet feed over working ZSM-5 (135) catalysts



**Figure 4:** TPSR experiments with 5 vol% DME inlet feed over fresh ZSM-5 (36) catalysts



**Figure 5:** TPSR experiments with 5 vol% DME inlet feed over working ZSM-5 (36) catalysts

## 4. Discussion

### 4.1. The behaviour of DME in the presence or absence of reaction

A comparison of TPD profiles to TPSR profiles of DME over ZSM-5 (36) and (135) catalysts is given in Figure 1. We note here that we are fitting experimental data with several reaction chemistries on different sites. Although we note that all elementary steps will be important in fitting the experimental data, not all are relevant over each active/binding site. On site 1 over fresh and working ZSM-5 (135), methanol dissociative adsorption, DME dissociative adsorption and reversible molecular adsorption, and methoxymethyl formation are relevant. In comparison, over site 6, further elementary steps are involved such as methanol molecular adsorption, formation of dimethoxyethane and methyl propenyl ether. On site 1 over fresh and working ZSM-5 (36), methanol dissociative adsorption, DME dissociative adsorption, and reversible molecular adsorption as well as methoxy methyl formation are relevant. In comparison, methanol molecular and reversible dissociative adsorption, DME dissociative adsorption and desorption, methoxymethyl formation, dimethoxyethane formation, methyl propenyl ether formation and propylene formation are relevant over site 6. Nonetheless, on both fresh and working catalysts, the reaction steps are consistent, and the activation energies increase systematically from low energy sites (site 1) to high energy sites (site 6). Consistency of reaction steps across the different sites would lead to an explosion in the number of parameters to be fitted and cross-correlation between the parameters. Thus, according to the microkinetic method proposed by Dumesic et al.<sup>77,78</sup>, the desire to include all reaction intermediates on the catalyst surface is balanced with the need to express the mechanism in terms of kinetic parameters that are accessible to experimental measurements or theoretical prediction. This compromise between the mechanistic detail and kinetic parameter estimation plays an important role in the use of microkinetic analysis for catalytic reaction synthesis.

### 4.2. Comparison of fresh to working catalysts

On fresh ZSM-5 (135) catalysts, 0.28% of the overall sites are used in the transformation of DME, while on working ZSM-5 (135) catalysts, 0.32% of the overall sites are used. Over fresh

ZSM-5 (36) catalysts, 0.84% of the overall sites are used and over working ZSM-5 (36), 0.82% of the overall sites are used. The active sites are a minority of the total binding sites. More sites are used in working ZSM-5 (135) catalysts for the TPSR of DME compared to fresh ZSM-5 (135) catalysts.

Over ZSM-5 (135) catalysts, there are three adsorption and desorption sites (Sites 2, 3 and 4) and the other sites allow for the formation of intermediates. The activation energies of desorption of DME over these adsorption/desorption (AD) sites are generally higher over the working catalysts compared to the fresh catalysts. A similar activation energy of the dissociative adsorption of DME over site 3 for fresh and working catalyst is obtained. Although, the number of binding AD sites are lower over working ZSM-5 (135) sites in comparison to fresh ZSM-5 (135) sites, the number of adsorption/desorption/reaction (ADR) sites are generally higher over working ZSM-5 (135) in comparison to fresh ZSM-5 (135) sites. Consequently, the total number of binding/active sites over working ZSM-5 (135) are higher than fresh ZSM-5 (135) catalysts. On the ADR sites, the activation energies of desorption and reaction are generally higher over working ZSM-5 (135) catalysts. On all sites, non-activated adsorption is obtained.

Over ZSM-5 (36) catalysts, there are three adsorption and desorption sites (sites 1, 2 and 3) and the remaining sites allow for the formation of propylene. Sites 1, 2 and 3 are binding sites (AD) while all other sites are active (ADR). On the AD sites, the activation energy of desorption of DME over working catalysts is generally similar to that of fresh catalysts. On ADR sites, activation energies are generally higher over working compared to fresh ZSM-5 (36) catalysts. As we observed for ZSM-5 (135), the site densities are generally higher over working ZSM-5 (36) catalysts compared to fresh ZSM-5 (36) catalysts. On all sites, non-activated adsorption is also obtained.

The activation energies over ZSM-5 (36) are generally higher than ZSM-5 (135) catalysts over ADR sites for propylene formation in the temperature range investigated. It is important to note that no propylene is formed over ZSM-5 (135) catalysts over the temperature range (300 – 723 K) used at  $15 \text{ K min}^{-1}$ . Given the lower concentration of Brønsted acid sites in ZSM-5 (135) catalysts (see section 2.3), it is plausible that much higher temperatures are required to produce

propylene, which would lead to higher activation energies than those obtained with ZSM-5 (36) catalysts, as expected. Interestingly, we observe that propylene formation on the most energetic sites requires activation energies of *ca.* 200 kJ mol<sup>-1</sup> over ZSM-5 (36) catalysts. This activation energy observed over ZSM-5 catalysts in our study is different from those observed from Li et al.<sup>37</sup> over SAPO-34 catalysts (135 kJ mol<sup>-1</sup>). This is probably due to the differing steric constraints associated with the intermediates in SAPO-34 and ZSM-5 catalysts. It does however show that SAPO-34 catalysts require less energy to produce propylene compared to ZSM-5 catalysts and justifies the current industrial application.<sup>79</sup> Also, there are subtle differences in the reaction mechanism used in our kinetic modelling study and the modelling conducted on the microscale using density functional theory calculations by Li et al.<sup>37</sup> This choice in the reduction of reaction steps is to reduce cross-correlation between parameters representing such steps while being able to explain the trends in experimental data as explained in the method by Dumesic.<sup>78</sup>

We observe scaling relations between the activation energies of dissociative desorption of DME and the formation of methoxy methyl species and methyl propenyl ether over sites 5 and 6, respectively (Figure 6) in fresh and working ZSM-5 catalysts. As shown above, the methoxy methyl cation and methyl propenyl ether species are not produced over site 4 of ZSM-5 (135) catalysts. We find the desorption energies of DME as an activity descriptor over ZSM-5 catalysts.

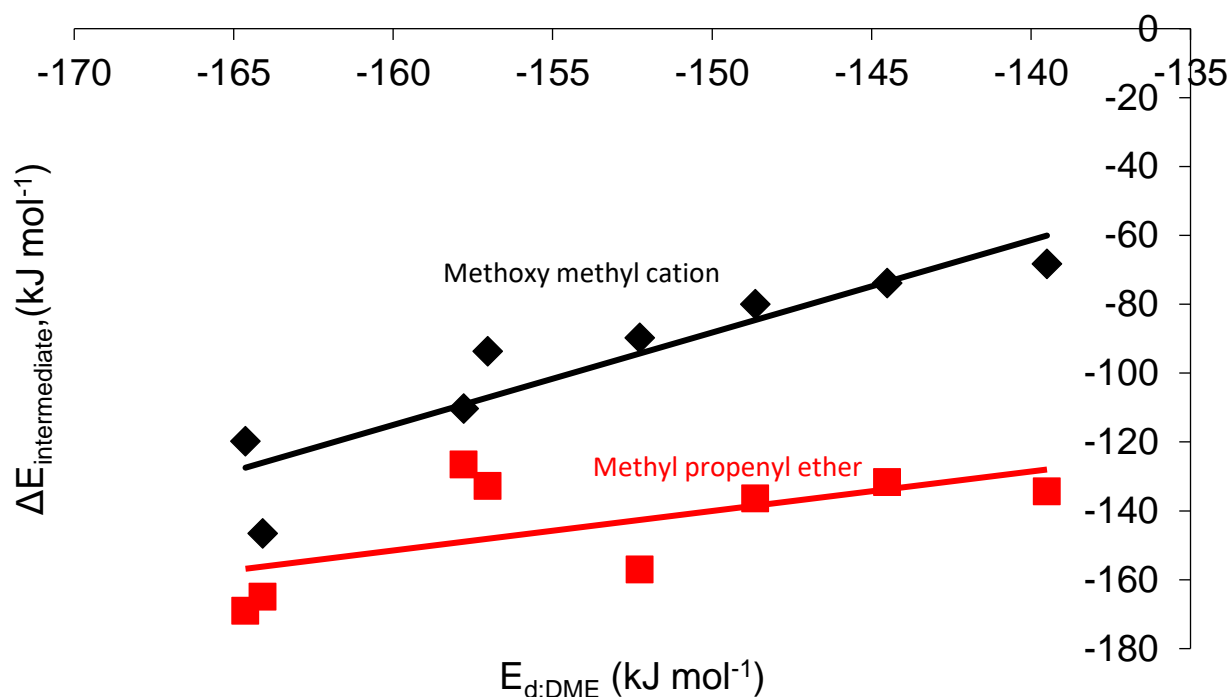


**Figure 6:** Scaling relations between the formation barriers of reaction intermediates of propylene formation as a function of activation energies of desorption of DME over sites 5 and 6 of fresh and working ZSM-5 (36) and ZSM-5 (135) catalysts

#### 4.3. The reductionist and integrated approach to DTO catalysis

The direct formation of olefins has been considered a highly energetic process requiring energies *ca.* 200 kJ mol<sup>-1</sup>.<sup>80,81</sup> Cluster models (1T, 3T, 5T) and periodic calculations for the methane-formaldehyde mechanism gave critical energy barriers of 171, 185, 183.1, 149.6 kJ mol<sup>-1</sup> respectively.<sup>37</sup> We uncover here that the formation of propylene over ZSM-5 catalysts through a direct mechanism requires similar activation energies. The activation energies also compare favourably with recent studies by Cordero-Lanzac et al. over ZSM-5 catalysts.<sup>82</sup> The TPSR studies over ZSM-5 (135) and (36) catalysts show that activation energies are generally higher over working catalysts than fresh catalysts. This implies that on DME introduction into the reactor, it is at first relatively easier to carry out AD and ADR reactions. However, during steady state where a working catalyst is established, the energies of desorption and reaction are relatively higher. Possible surface reconstruction or the formation of layers of adsorption species

on the ZSM-5 catalysts occurs with the formation of a working catalyst. Such a change in the surface properties of the ZSM-5 catalyst could lead to a change in the desorption and reaction energies. Maintaining a state of temperature modulation into the reactor, by systematically desorbing products off the catalyst pores i.e. purging such layers off the catalyst surface or through the addition of another component, could increase the activity of DME over ZSM-5 catalysts. Indeed, process modulation for increasing activity has been observed<sup>83</sup>, although the mechanism governing the modulation process has not been adequately explained.<sup>46</sup>

The Taylor site model<sup>84</sup> is further evinced given the lower number of binding/active sites involved in DME transformation to propylene (< 1%) over all catalysts. We note that higher number of binding/active working sites are obtained compared to fresh sites suggesting that, perhaps, increasing mesoporosity allowing for higher access to binding sites is obtained for working ZSM-5 catalysts in accordance to previous studies by Howe et al.<sup>85</sup>

In the reductionist approach where we studied the adsorption, desorption, diffusion, and reaction of DME over ZSM-5 catalysts of different Si/Al ratios individually, we observed that DME has higher surface coverages and higher activation energies of desorption than methanol. We also observed higher activation energies of desorption over ZSM-5 (135) compared to ZSM-5 (36).<sup>51,61</sup> Higher DME self-diffusion coefficients were observed over ZSM-5 (135) compared to ZSM-5 (36).<sup>52</sup> The mobility of DME diffusion through ZSM-5 catalysts does not limit either the TPD or TPSR studies. We observed activation energies of DME diffusion of 0.96 and 1.33 kJ mol<sup>-1</sup> over fresh ZSM-5 (36) and (135) catalysts, respectively. Dispersion through the bed in the reactor (10<sup>-9</sup> m<sup>2</sup> s<sup>-1</sup>) is much faster than DME diffusion through the catalyst particles (10<sup>-10</sup> m<sup>2</sup> s<sup>-1</sup>) suggesting that catalyst particles act as hot centres within the reactor bed.<sup>48,52</sup> Other factors such as pore length distribution and velocity profile could play a role.<sup>86</sup> We obtained evidence that the methoxymethyl pathway gives the best evidence to experimental data (during the induction period) amongst all other pathways tested (including carbon monoxide, methane-formaldehyde).<sup>48</sup> We do note further that the methoxymethyl pathway only explains the induction period during which the first C-C bond is formed. We expect a better fit to experimental data the chemistries governing the transition regime and the steady state is included especially as

methanol begins to portray steady-state behaviour even during the temperature transient. The chemistries governing the transition regime and steady state are dependent on the process conditions and Si/Al ratio. Under vacuum or close to vacuum conditions, there is as of yet limited studies on the existence of a hydrocarbon pool. Further analysis of the carbene mechanism (section S8) shows its unsuitability to explain the primary formation of olefins during the induction period. We do envisage that accounting for the chemistries of the induction period, transition regime and steady-state conditions would involve many species, which may require advanced methods to obtain activity descriptors during methanol-to-olefin conversion.

Using the integrated approach in this study where adsorption, desorption, and reaction of DME over ZSM-5 catalysts of different Si/Al ratios is investigated, we observe that the working catalyst requires higher energies compared to fresh catalysts. Also, by comparing the desorption of DME to methanol individually through their temperature programmed desorption, we observed higher activation energies of desorption of DME compared to methanol across all sites (see supplementary information in ref<sup>51</sup>). In the integrated approach used in this TPSR study, over ZSM-5 (36) catalysts, we also obtain that the activation energies of desorption of DME is higher than methanol over ADR sites 4, 5 and 6, thereby corroborating our initial thesis obtained using the reductionist approach.

#### 4.4. Bridging vacuum and atmospheric studies during dimethyl ether to olefin conversion

For the conversion of DME over working ZSM-5 (135) catalysts, we observed a rate of transformation of  $ca. 10^{-6} \text{ mol}_{\text{DME}} \text{ m}_{\text{cat}}^{-3} \text{ s}^{-1}$  (TOF =  $3.63 \times 10^{-6} \text{ s}^{-1}$ ) at pressures of  $10^{-5} \text{ Pa}$  ( $1 \times 10^{-10} \text{ bar}$ ). Perez-Uriarte et al.<sup>14</sup> observed rates of DME transformation over ZSM-5 (140) catalysts of  $ca. 0.38 \text{ mol}_{\text{DME}} \text{ m}_{\text{cat}}^{-3} \text{ s}^{-1}$  in a fixed bed reactor at  $ca. 1 \text{ bar}$  (TOF =  $1.38 \text{ s}^{-1}$ ). The pressure gap of  $10^{10} \text{ bar}$  gives rise to a transformational activity gap of  $10^5$ . The aforementioned pressure gap may be due to the different rate constants and order of reaction. For a pure feed, assuming first order reaction with DME over working ZSM-5 catalysts, there is no expectation to the change in order by mass transfer limitation. The activation energy for olefin formation (i.e. propylene) is observed to be  $ca. 200 \text{ kJ mol}^{-1}$ . The activation energies for olefin formation are similar to DFT

calculations reported by Lesthaeghe et al. in other direct mechanisms.<sup>80,81</sup> Given the similarities between our vacuum studies and DFT studies, we infer that our activation energies are intrinsic for the formation of primary olefins. Perez-Uriarte et al. reported kinetics during DME transformation to olefins over ZSM-5 (140) catalysts of 42 kJ mol<sup>-1</sup> under atmospheric conditions.<sup>14</sup> Considering the activation energies obtained from both vacuum studies and atmospheric studies, it is likely that the atmospheric studies carried out by Perez-Uriarte et al.<sup>14</sup> are under mass transfer limitations. Nonetheless, the same group has reported higher activation energies for DME transformation to olefins<sup>82</sup>, which agree with our current work.

#### 4.5. Sensitivity analysis

To assess site-specific information on activity promoters and inhibitors during the DME TPSR over ZSM-5 catalysts, each parameter was multiplied by a perturbation factor of 0.2 while the other rate parameters were kept constant. The relative changes in desorption profiles were obtained with or without the perturbation factor. Subsequently, the sensitivity coefficient was obtained as presented in equation 2.6:

$$K_s = \frac{\ln(Y_p/Y_o)}{\ln(F)} \quad (2.6)$$

where  $Y_p$  and  $Y_o$  are the rates with and without perturbation and  $F$  is the perturbation factor. The TPSR of DME over fresh ZSM-5 (36) catalysts is illustrated here as an example.

The sensitivity analysis (Figure 7) shows that several steps are important. We observed that the most important parameter is the desorption of DME over site 4. A lower perturbation factor had to be applied to give similar sensitivities from other parameters. As shown in Figure 6, the desorption of DME is a descriptor governing the activity of ZSM-5 catalysts for olefin production.

According to the sensitivity analysis, most elementary steps promote the activity of DME transformation to olefins. We observe that site 4 has the highest density of rate determining steps. Efforts to promote catalyst design for the transformation of dimethyl ether to olefins should focus

on its functionality, that is on moderately high temperature AD/ADR sites operating between 450 and 600 K.



**Figure 7:** Sensitivity coefficient of rate parameters obtained for DME TPSR over fresh ZSM-5 (36) catalysts

#### 4.6. Nature of Binding and Active Sites

During DME TPSR over fresh catalysts, the catalyst is transformed from a fresh catalyst to a working catalyst (state A). During DME TPSR over working catalysts, the catalyst is transformed from a working catalyst (state B, obtained under atmospheric conditions) to another working state (state C, influenced by vacuum studies). At low temperatures, during the linear temperature ramp, only some sites on the quasi-fresh catalyst are involved (site 1). At high temperatures, site 6 is activated. Our model assumes static sites across these states and does not provide information on the location of these sites. A complexity due to active site dynamics has been highlighted recently.<sup>87-89</sup> However, such nuanced descriptions have not been included in our model and are beyond the scope of this current work and will be considered in a coming publication.

Nonetheless, in this non-linear model of coupled partial differential equations, we observe good agreement between experiment and model, especially in the induction period. In this static model, six sites are observed. The mathematical model allows for only specification of Brønsted acid sites. Yarulina et al.<sup>90</sup> observed that the isolation of Brønsted acid sites is key to the selective formation of propylene. Lewis sites prevent the formation of coke, thus increasing catalyst lifetime. As such in this kinetic modelling study, only Brønsted acid sites have been considered. Six kinds of Brønsted acid sites are activated with increase in temperature and time on stream. While it is widely agreed that there is one type of Brønsted acid site (here represented as HZ), our model allowing for six kinds of these Brønsted acid sites highlights non-uniformity of this type of Brønsted acid site and will be subject to further investigation in our future work.

#### 5. Conclusions

The conversion of dimethyl ether to olefins over fresh and working ZSM-5 catalysts of different Si/Al ratios has been studied using a combination of temperature programmed surface reaction experiments and microkinetic modelling. The methoxymethyl pathway involving dimethoxyethane and methyl propenyl ether has been used to describe the kinetics

of dimethyl ether conversion to olefins in the induction period. We unravel six ensembles of binding/active sites. Three of these sites were strictly associated with adsorption/desorption while the remaining three were associated with adsorption/desorption/reaction. These six ensembles of binding sites account for less than 1% of the total amount of sites present on the catalyst. Barriers of activation energies of desorption, and surface reaction change between fresh and working catalysts and different Si/Al ratios, probably due to changing porosity and formation of adspecies which changes the surface properties with time on stream. Reaction barriers obtained during the temperature programmed surface reaction experiments of DME agree closely with archived density functional theory calculations. The desorption energies of dimethyl ether serve as a descriptor for activity over ZSM-5 catalysts as we observe scaling relations with the formation of key intermediates (methoxy methyl species and methyl propenyl ether) leading to propylene formation.

## 6. Declaration of Interest

There are no conflicts of interest to declare.

## 7. Acknowledgements

Financial support from the Petroleum Technology Development Fund of Nigeria (PTDF/ED/PHD/OO/766/15) and from the European Commission in the scope of the 7th Framework program BIOGO project (grant number: 604296) <https://www.biogo.eu/> is acknowledged. Toyin Omojola thanks Dr. Dmitry Lukyanov for fruitful scientific discussions.

## 8. Supplementary Information

Relevant details about sample TPSR profile, quantitative analysis procedure, full DME TPSR profiles over ZSM-5 catalysts, kinetic parameters of adsorption, desorption, and surface reaction over ZSM-5 (36) and (135) catalysts, gaussian fits, parity plots, carbene mechanism are given in the supplementary information.

## 9. References

- (1) Amghizar, I.; Vandewalle, L. A.; Van Geem, K. M.; Marin, G. B. New Trends in Olefin Production. *Engineering* **2017**, *3*, 171-178.
- (2) Vora, B. V.; Marker, T. L.; Barger, P. T.; Nilsen, H. R.; Kvisle, S.; Fuglerud, T.: Economic route for natural gas conversion to ethylene and propylene. In *Stud. Surf. Sci. Catal.*; Pontes, M. d., Espinoza, R. L., Nicolaidis, C. P., Scholtz, J. H., Scurrrell, M. S., Eds.; Elsevier, 1997; Vol. Volume 107; pp 87-98.
- (3) Chang, C. D.; Chu, C. T. W.; Socha, R. F. Methanol conversion to olefins over ZSM-5: I. Effect of temperature and zeolite SiO<sub>2</sub>Al<sub>2</sub>O<sub>3</sub>. *J. Catal.* **1984**, *86*, 289-296.
- (4) Chu, C. T. W.; Chang, C. D. Methanol conversion to olefins over ZSM-5. II. Olefin distribution. *J. Catal.* **1984**, *86*, 297-300.
- (5) Inoue, Y.; Nakashiro, K.; Ono, Y. Selective conversion of methanol into aromatic hydrocarbons over silver-exchanged ZSM-5 zeolites. *Microporous Mater.* **1995**, *4*, 379-383.
- (6) Chang, C. D.; Silvestri, A. J. The conversion of methanol and other O-compounds to hydrocarbons over zeolite catalysts. *J. Catal.* **1977**, *47*, 249-259.
- (7) O'Malley, A.; Parker, S. F.; Chutia, A.; Farrow, M. R.; Silverwood, I. P.; Garcia-Sakai, V.; Catlow, C. R. A. Room temperature methoxylation in zeolites: insight into a key step of the methanol-to-hydrocarbons process. *ChemComm* **2016**, *52*, 2897-2900.
- (8) Matam, S. K.; Howe, R. F.; Thetford, A.; Catlow, C. R. A. Room temperature methoxylation in zeolite H-ZSM-5: an operando DRIFTS/mass spectrometric study. *Chem. Commun.* **2018**, *54*, 12875-12878.
- (9) Wang, W.; Seiler, M.; Hunger, M. Role of surface methoxy species in the conversion of methanol to dimethyl ether on acidic zeolites investigated by in situ stopped-flow MAS NMR spectroscopy. *J. Phys. Chem. B* **2001**, *105*, 12553-12558.
- (10) Svelle, S.; Kolboe, S.; Swang, O.; Olsbye, U. Methylation of Alkenes and Methylbenzenes by Dimethyl Ether or Methanol on Acidic Zeolites. *The Journal of Physical Chemistry B* **2005**, *109*, 12874-12878.

- (11) Omojola, T.; Cherkasov, N.; Rebrov, E. V.; Lukyanov, D. B.; Perera, S. P. Zeolite minilith: A unique structured catalyst for the methanol to gasoline process. *Chemical Engineering and Processing-Process Intensification* **2018**, *131*, 137-143.
- (12) Ateka, A.; Rodriguez-Vega, P.; Cordero-Lanzac, T.; Bilbao, J.; Aguayo, A. T. Model validation of a packed bed LTA membrane reactor for the direct synthesis of DME from CO/CO<sub>2</sub>. *Chem. Eng. J.* **2020**.
- (13) Ereña, J.; Sierra, I.; Aguayo, A. T.; Ateka, A.; Olazar, M.; Bilbao, J. Kinetic modelling of dimethyl ether synthesis from (H<sub>2</sub>+CO<sub>2</sub>) by considering catalyst deactivation. *Chem. Eng. J.* **2011**, *174*, 660-667.
- (14) Pérez-Urriarte, P.; Ateka, A.; Aguayo, A. T.; Gayubo, A. G.; Bilbao, J. Kinetic model for the reaction of DME to olefins over a HZSM-5 zeolite catalyst. *Chem. Eng. J.* **2016**, *302*, 801-810.
- (15) Pérez-Urriarte, P.; Gamero, M.; Ateka, A.; Díaz, M.; Aguayo, A. T.; Bilbao, J. Effect of the Acidity of HZSM-5 Zeolite and the Binder in the DME Transformation to Olefins. *Ind. Eng. Chem. Res.* **2016**, *55*, 1513-1521.
- (16) Dahl, I. M.; Kolboe, S. On the Reaction Mechanism for Hydrocarbon Formation from Methanol over SAPO-34. I. Isotopic Labeling Studies of the Co-Reaction of Ethene and Methanol. *J. Catal.* **1994**, *149*, 458-464.
- (17) Dahl, I. M.; Kolboe, S. On the reaction mechanism for hydrocarbon formation from methanol over SAPO-34: 2. Isotopic labeling studies of the Co-reaction of propene and methanol. *J. Catal.* **1996**, *161*, 304-309.
- (18) Dahl, I. M.; Kolboe, S. On the reaction mechanism for propene formation in the MTO reaction over SAPO-34. *Catal. Lett.* **1993**, *20*, 329-336.
- (19) Olsbye, U.; Bjørgen, M.; Svelle, S.; Lillerud, K. P.; Kolboe, S. Mechanistic insight into the methanol-to-hydrocarbons reaction. *International Conference on Gas-Fuel 05* **2005**, *106*, 108-111.

(20) Bjørgen, M.; Svelle, S.; Joensen, F.; Nerlov, J.; Kolboe, S.; Bonino, F.; Palumbo, L.; Bordiga, S.; Olsbye, U. Conversion of methanol to hydrocarbons over zeolite H-ZSM-5: On the origin of the olefinic species. *J. Catal.* **2007**, *249*, 195-207.

(21) Bjørgen, M.; Joensen, F.; Lillerud, K. P.; Olsbye, U.; Svelle, S. The mechanisms of ethene and propene formation from methanol over high silica H-ZSM-5 and H-beta. *Catal. Today* **2009**, *142*, 90-97.

(22) Müller, S.; Liu, Y.; Kirchberger, F. M.; Tonigold, M.; Sanchez-Sanchez, M.; Lercher, J. A. Hydrogen Transfer Pathways during Zeolite Catalyzed Methanol Conversion to Hydrocarbons. *Journal of the American Chemical Society* **2016**, *138*, 15994-16003.

(23) Takahashi, A.; Xia, W.; Wu, Q.; Furukawa, T.; Nakamura, I.; Shimada, H.; Fujitani, T. Difference between the mechanisms of propylene production from methanol and ethanol over ZSM-5 catalysts. *Applied Catalysis A: General* **2013**, *467*, 380-385.

(24) Koempel, H.; Liebner, W.: Lurgi's Methanol To Propylene (MTP®) Report on a successful commercialisation. In *Stud. Surf. Sci. Catal.*, 2007; Vol. 167; pp 261-267.

(25) Chang, C. D.; Lang, W. H.; Smith, R. L. The conversion of methanol and other O-compounds to hydrocarbons over zeolite catalysts. II. Pressure effects. *J. Catal.* **1979**, *56*, 169-173.

(26) Yamazaki, H.; Shima, H.; Imai, H.; Yokoi, T.; Tatsumi, T.; Kondo, J. N. Evidence for a "carbene-like" intermediate during the reaction of methoxy species with light alkenes on H-ZSM-5. *Angewandte Chemie - International Edition* **2011**, *50*, 1853-1856.

(27) Wang, W.; Hunger, M. Reactivity of surface alkoxy species on acidic zeolite catalysts. *Acc. Chem. Res.* **2008**, *41*, 895-904.

(28) Jiang, Y.; Hunger, M.; Wang, W. On the reactivity of surface methoxy species in acidic zeolites. *Journal of the American Chemical Society* **2006**, *128*, 11679-11692.

(29) Yamazaki, H.; Shima, H.; Imai, H.; Yokoi, T.; Tatsumi, T.; Kondo, J. N. Direct production of propene from methoxy species and dimethyl ether over H-ZSM-5. *Journal of Physical Chemistry C* **2012**, *116*, 24091-24097.

(30) Chowdhury, A. D.; Houben, K.; Whiting, G. T.; Mokhtar, M.; Asiri, A. M.; Al-Thabaiti, S. A.; Basahel, S. N.; Baldus, M.; Weckhuysen, B. M. Initial Carbon–Carbon Bond Formation during the Early Stages of the Methanol-to-Olefin Process Proven by Zeolite-Trapped Acetate and Methyl Acetate. *Angewandte Chemie - International Edition* **2016**, *55*, 15840-15845.

(31) Lesthaeghe, D.; Van Speybroeck, V.; Marin, G. B.; Waroquier, M. What role do oxonium ions and oxonium ylides play in the ZSM-5 catalysed methanol-to-olefin process? *Chem. Phys. Lett.* **2006**, *417*, 309-315.

(32) Hutchings, G. J.; Gottschalk, F.; Hall, M. V. M.; Hunter, R. Hydrocarbon formation from methylating agents over the zeolite catalyst ZSM-5. Comments on the mechanism of carbon-carbon bond and methane formation. *Journal of the Chemical Society, Faraday Transactions 1: Physical Chemistry in Condensed Phases* **1987**, *83*, 571-583.

(33) Wu, X.; Xu, S.; Zhang, W.; Huang, J.; Li, J.; Yu, B.; Wei, Y.; Liu, Z. Direct Mechanism of the First Carbon–Carbon Bond Formation in the Methanol-to-Hydrocarbons Process. *Angew. Chem. Int. Ed.* **2017**, *56*, 9039-9043.

(34) Wang, W.; Buchholz, A.; Seiler, M.; Hunger, M. Evidence for an Initiation of the Methanol-to-Olefin Process by Reactive Surface Methoxy Groups on Acidic Zeolite Catalysts. *Journal of the American Chemical Society* **2003**, *125*, 15260-15267.

(35) Jiang, Y.; Wang, W.; Marthala, V. R. R.; Huang, J.; Sulikowski, B.; Hunger, M. Effect of organic impurities on the hydrocarbon formation via the decomposition of surface methoxy groups on acidic zeolite catalysts. *J. Catal.* **2006**, *238*, 21-27.

(36) Jiang, Y.; Wang, W.; Reddy Marthala, V. R.; Huang, J.; Sulikowski, B.; Hunger, M. Response to comments on the paper: "Effect of organic impurities on the hydrocarbon formation via the decomposition of surface methoxy groups on acidic zeolite catalysts" by Y. Jiang, W. Wang, V.R.R. Marthala, J. Huang, B. Sulikowski, M. Hunger. *J. Catal.* **2006**, *244*, 134-136.

(37) Li, J.; Wei, Z.; Chen, Y.; Jing, B.; He, Y.; Dong, M.; Jiao, H.; Li, X.; Qin, Z.; Wang, J.; Fan, W. A route to form initial hydrocarbon pool species in methanol conversion to olefins over zeolites. *J. Catal.* **2014**, *317*, 277-283.

(38) Wei, Z.; Chen, Y. Y.; Li, J.; Guo, W.; Wang, S.; Dong, M.; Qin, Z.; Wang, J.; Jiao, H.; Fan, W. Stability and Reactivity of Intermediates of Methanol Related Reactions and C-C Bond Formation over H-ZSM-5 Acidic Catalyst: A Computational Analysis. *Journal of Physical Chemistry C* **2016**, *120*, 6075-6087.

(39) Olsbye, U.; Svelle, S.; Lillerud, K. P.; Wei, Z. H.; Chen, Y. Y.; Li, J. F.; Wang, J. G.; Fan, W. B. The formation and degradation of active species during methanol conversion over protonated zeotype catalysts. *Chem. Soc. Rev.* **2015**, *44*, 7155-7176.

(40) McCarty, J. G.; Wise, H. Hydrogenation of surface carbon on alumina-supported nickel. *J. Catal.* **1979**, *57*, 406-416.

(41) Zijlstra, B.; Broos, R. J. P.; Chen, W.; Filot, I. A. W.; Hensen, E. J. M. First-principles based microkinetic modeling of transient kinetics of CO hydrogenation on cobalt catalysts. *Catal. Today* **2020**, *342*, 131-141.

(42) Haure, P. M.; Hudgins, R. R.; Silveston, P. L. Periodic operation of a trickle-bed reactor. *AIChE J.* **1989**, *35*, 1437-1444.

(43) Cutlip, M. B.; Hawkins, C. J.; Mukesh, D.; Morton, W.; Kenney, C. N. Modelling of forced periodic oscillations of carbon monoxide oxidation over platinum catalyst. *Chem. Eng. Commun.* **1983**, *22*, 329-344.

(44) Hegedus, L. L.; Chang, C. C.; McEwen, D. J.; Sloan, E. M. Response of Catalyst Surface Concentrations to Forced Concentration Oscillations in the Gas Phase. The NO, CO, O. System over Pt-Alumina. *Ind. Eng. Chem. Fundam.* **1980**, *19*, 367-373.

(45) Imbihl, R.; Ertl, G. Oscillatory Kinetics in Heterogeneous Catalysis. *Chem. Rev.* **1995**, *95*, 697-733.

(46) Thomas, J. M.; Thomas, W. J.: *Principles and Practice of Heterogeneous Catalysis* 2nd ed.; Wiley-VCH: Weinheim, Germany, 2015.

(47) Wright, P. A.: *Microporous framework solids*; RSC: Cambridge, 2008.

(48) Omojola, T.; Lukyanov, D. B.; van Veen, A. C. Transient kinetic studies and microkinetic modeling of primary olefin formation from dimethyl ether over ZSM-5 catalysts. *Int. J. Chem. Kinet.* **2019**, *51*, 528-537.

(49) Omojola, T.; Lukyanov, D. B.; Cherkasov, N.; Zholobenko, V. L.; van Veen, A. C. Influence of Precursors on the Induction Period and Transition Regime of Dimethyl Ether Conversion to Hydrocarbons over ZSM-5 Catalysts. *Industrial & Engineering Chemistry Research* **2019**, *58*, 16479-16488.

(50) Li, Y.; Zhang, M.; Wang, D.; Wei, F.; Wang, Y. Differences in the methanol-to-olefins reaction catalyzed by SAPO-34 with dimethyl ether as reactant. *J. Catal.* **2014**, *311*, 281-287.

(51) Omojola, T.; Cherkasov, N.; McNab, A. I.; Lukyanov, D. B.; Anderson, J. A.; Rebrov, E. V.; van Veen, A. C. Mechanistic Insights into the Desorption of Methanol and Dimethyl Ether Over ZSM-5 Catalysts. *Catal. Lett.* **2018**, *148*, 474-488.

(52) Omojola, T.; Silverwood, I. P.; O'Malley, A. J. Molecular behaviour of methanol and dimethyl ether in H-ZSM-5 catalysts as a function of Si/Al ratio: a quasielastic neutron scattering study. *Catalysis Science & Technology* **2020**, *10*, 4305-4320.

(53) Gleaves, J. T.; Ebner, J. R.; Kuechler, T. C. Temporal Analysis of Products (TAP) — A Unique Catalyst Evaluation System with Submillisecond Time Resolution. *Catalysis Reviews* **1988**, *30*, 49-116.

(54) Yablonsky, G. S.; Olea, M.; Marin, G. B. Temporal analysis of products: basic principles, applications, and theory. *J. Catal.* **2003**, *216*, 120-134.

(55) Gleaves, J. T.; Yablonsky, G.; Zheng, X.; Fushimi, R.; Mills, P. L. Temporal analysis of products (TAP)—Recent advances in technology for kinetic analysis of multi-component catalysts. *J. Mol. Catal. A: Chem.* **2010**, *315*, 108-134.

(56) Morgan, K.; Maguire, N.; Fushimi, R.; Gleaves, J. T.; Goguet, A.; Harold, M. P.; Kondratenko, E. V.; Menon, U.; Schuurman, Y.; Yablonsky, G. S. Forty years of temporal analysis of products. *Catalysis Science and Technology* **2017**, *7*.

(57) Van Veen, A. C.; Zanthoff, H. W.; Hinrichsen, O.; Muhler, M. Fixed-bed microreactor for transient kinetic experiments with strongly adsorbing gases under high vacuum conditions. *Journal of Vacuum Science and Technology, Part A: Vacuum, Surfaces and Films* **2001**, *19*, 651-655.

(58) Rao, S. M.; Saraçi, E.; Gläser, R.; Coppens, M. O. Surface barriers as dominant mechanism to transport limitations in hierarchically structured catalysts - Application to the zeolite-catalyzed alkylation of benzene with ethylene. *Chem. Eng. J.* **2017**.

(59) Haw, J. F.; Song, W.; Marcus, D. M.; Nicholas, J. B. The Mechanism of Methanol to Hydrocarbon Catalysis. *Acc. Chem. Res.* **2003**, *36*, 317-326.

(60) Marin, G. B.; Yablonsky, G. S.: *Kinetics of Chemical Reactions: Decoding Complexity* WILEY-VCH: Weinheim, Germany, 2011.

(61) Omojola, T.; van Veen, A. C. Competitive adsorption of oxygenates and aromatics during the initial steps of the formation of primary olefins over ZSM-5 catalysts. *Catal. Commun.* **2020**, *140*.

(62) Courant, R.; Friedrichs, K.; Lewy, H. Über die partiellen Differenzgleichungen der mathematischen Physik. *Mathematische Annalen* **1928**, *100*, 32-74.

(63) Hunger, B.; Matysik, S.; Heuchel, M.; Einicke, W. D. Adsorption of methanol on ZSM-5 zeolites. *Langmuir* **1997**, *13*, 6249-6254.

(64) Hunger, B.; Matysik, S.; Heuchel, M.; Geidel, E.; Toufar, H. Adsorption of water on zeolites of different types. *J. Therm. Anal.* **1997**, *49*, 553-565.

(65) Hunger, B.; Heuchel, M.; Matysik, S.; Beck, K.; Einicke, W. D. Adsorption of water on ZSM-5 zeolites. *Thermochim. Acta* **1995**, *269-270*, 599-611.

(66) Van Der Linde, S. C.; Nijhuis, T. A.; Dekker, F. H. M.; Kapteijn, F.; Moulijn, J. A. Mathematical treatment of transient kinetic data: Combination of parameter estimation with solving the related partial differential equations. *Applied Catalysis A: General* **1997**, *151*, 27-57.

(67) Rasmuson, A.; Andersson, B.; Olsson, L.; Andersson, R.: *Mathematical Modeling in Chemical Engineering* Cambridge University Press: USA, 2014.

(68) Lagarias, J. C.; Reeds, J. A.; Wright, M. H.; Wright, P. E. Convergence properties of the Nelder-Mead simplex method in low dimensions. *SIAM Journal on Optimization* **1998**, *9*, 112-147.

(69) Gayubo, A. G.; Alonso, A.; Valle, B.; Aguayo, A. T.; Bilbao, J. Kinetic Model for the Transformation of Bioethanol into Olefins over a HZSM-5 Zeolite Treated with Alkali. *Industrial & Engineering Chemistry Research* **2010**, *49*, 10836-10844.

(70) Zhang, W.; Zhi, Y.; Huang, J.; Wu, X.; Zeng, S.; Xu, S.; Zheng, A.; Wei, Y.; Liu, Z. Methanol to Olefins Reaction Route Based on Methylcyclopentadienes as Critical Intermediates. *ACS Catalysis* **2019**, *9*, 7373-7379.

(71) Kumar, P.; Thybaut, J. W.; Svelle, S.; Olsbye, U.; Marin, G. B. Single-event microkinetics for methanol to olefins on H-ZSM-5. *Ind. Eng. Chem. Res.* **2013**, *52*, 1491-1507.

(72) Schlögl, R. Active Sites for Propane Oxidation: Some Generic Considerations. *Top. Catal.* **2011**, *54*, 627.

(73) Schlögl, R. Selective Oxidation: From a Still Immature Technology to the Roots of Catalysis Science. *Top. Catal.* **2016**, *59*, 1461-1476.

(74) Grasselli, R. K. Genesis of site isolation and phase cooperation in selective oxidation catalysis. *Top. Catal.* **2001**, *15*, 93-101.

(75) Hunger, B.; Hoffmann, J. Temperature-programmed surface reactions (TPSR) on heterogeneous surfaces. *J. Therm. Anal.* **1993**, *40*, 1347-1356.

(76) Hunger, B.; Hoffmann, J. Kinetic analysis of temperature-programmed surface reactions on porous catalysts. *J. Therm. Anal.* **1992**, *38*, 739-748.

(77) Motagamwala, A. H.; Dumesic, J. A. Microkinetic Modeling: A Tool for Rational Catalyst Design. *Chem. Rev.* **2020**.

(78) Dumesic, J. A.; Rudd, D. F.; Aparicio, L. M.; Rekoske, J. E.; Trevino, A. A.: *The Microkinetics of Heterogeneous Catalysis*; American Chemical Society: Washington D.C, 1993.

(79) Tian, P.; Wei, Y.; Ye, M.; Liu, Z. Methanol to olefins (MTO): From fundamentals to commercialization. *ACS Catalysis* **2015**, *5*, 1922-1938.

(80) Lesthaeghe, D.; Van Speybroeck, V.; Marin, G. B.; Waroquier, M. Understanding the failure of direct C-C coupling in the zeolite-catalyzed methanol-to-olefin process. *Angewandte Chemie - International Edition* **2006**, *45*, 1714-1719.

(81) Lesthaeghe, D.; Van Speybroeck, V.; Marin, G. B.; Waroquier, M. The rise and fall of direct mechanisms in methanol-to-olefin catalysis: An overview of theoretical contributions. *Ind. Eng. Chem. Res.* **2007**, *46*, 8832-8838.

(82) Cordero-Lanzac, T.; Aguayo, A. T.; Bilbao, J. Reactor-regenerator system for the dimethyl ether-to-olefins process over HZSM-5 catalysts: Conceptual development and analysis of the process variables. *Ind. Eng. Chem. Res.* **2020**, *59*, 14689-14702.

(83) Renken, A.; Hudgins, R. R.; Silveston, P. L.: Use of Modulation in Mechanistic Studies. In *Periodic Operation of Reactors*; Hudgins, R. R., Silveston, P. L., Eds.; Elsevier, 2013.

(84) Taylor, H. S. Fourth Report of the Committee on Contact Catalysis. *The Journal of Physical Chemistry* **1926**, *30*, 145-171.

(85) Matam, S. K.; O'Malley, A. J.; Catlow, C. R. A.; Suwardiyanto; Collier, P.; Hawkins, A. P.; Zachariou, A.; Lennon, D.; Silverwood, I.; Parker, S. F.; Howe, R. F. The effects of MTG catalysis on methanol mobility in ZSM-5. *Catalysis Science & Technology* **2018**, *8*, 3304-3312.

(86) Dayan, J.; Levenspiel, O. Longitudinal dispersion in packed beds of porous adsorbing solids. *Chem. Eng. Sci.* **1968**, *23*, 1327-1334.

(87) Schlögl, R. Heterogeneous Catalysis. *Angew. Chem. Int. Ed.* **2015**, *54*, 3465-3520.

(88) Sauer, J.; Freund, H.-J. Models in Catalysis. *Catal. Lett.* **2015**, *145*, 109-125.

(89) Freund, H. J.; Kühlenbeck, H.; Libuda, J.; Rupprechter, G.; Bäumer, M.; Hamann, H. Bridging the pressure and materials gaps between catalysis and surface science: clean and modified oxide surfaces. *Top. Catal.* **2001**, *15*, 201-209.

(90) Yarulina, I.; De Wispelaere, K.; Bailleul, S.; Goetze, J.; Radersma, M.; Abou-Hamad, E.; Vollmer, I.; Goesten, M.; Mezari, B.; Hensen, E. J. M.; Martínez-Espín, J. S.; Morten, M.; Mitchell, S.; Perez-Ramirez, J.; Olsbye, U.; Weckhuysen, B. M.; Van Speybroeck, V.; Kapteijn, F.; Gascon, J. Structure–performance descriptors and the role of Lewis acidity in the methanol-to-propylene process. *Nature Chemistry* **2018**, *10*, 804-812.